On the solar cycle dependence of the amplitude modulation characterizing the mid-latitude sporadic E layer diurnal periodicity

M. Pezzopane[1], A. Pignalberi[2,3], M. Pietrella[1]

[1]Istituto Nazionale di Geofisica e Vulcanologia, 00143, Roma, Italy

[2]Università di Bologna “Alma Mater Studiorum, 40126, Bologna, Italy

Correspondence to: M. Pezzopane (michael.pezzopane@ingv.it), Tel: +39 06 51860525, Fax: +39 06 51860397

A. Pignalberi (pignalberialessio@yahoo.it); M. Pietrella (marco.pietrella@ingv.it)

Abstract

Spectral analyses are employed to investigate how the diurnal periodicity of the critical frequency of the sporadic E (Es) layer varies with solar activity. The study is based on ionograms recorded at the ionospheric station of Rome (41.8°N, 12.5°E), Italy, from 1976 to 2009, a period of time covering three solar cycles. It was confirmed that the diurnal periodicity is always affected by an amplitude modulation with periods of several days, which is the proof that Es layers are affected indirectly by planetary waves through their nonlinear interaction with atmospheric tides at lower altitudes. The most striking features coming out from this study is however that this amplitude modulation is greater for high solar activity than for low solar activity.

Keywords: sporadic E layer; mid-latitude ionosphere; planetary waves; nonlinear interaction

1. Introduction

The mid-latitude sporadic E (Es) layers, whose characteristics have been deeply studied (see reviews by Whitehead, 1989; Mathews, 1998; Haldoupis, 2011, 2012), are thin and dense layers of plasma forming mostly between 90 and 130 km of altitude, an ionospheric region characterized by complicated dynamics and nonlinear plasma processes; the Es phenomenon is itself representative of the complex coupling between the neutral atmosphere and the ionosphere which occurs right in this region.

It is believed that the formation of Es is caused by vertical wind shears in the neutral horizontal winds. In fact, this particular wind geometry, along with the combined action of ion-neutral collisional coupling and geomagnetic Lorentz forcing, can compel the long-lived metallic ions to move vertically and converge into dense and thin plasma layers; these layers are typically located close to the convergence node of the neutral horizontal wind vertical profile. This vertical wind-shear mechanism was formulated in the early sixties studies mostly associated with atmospheric gravity waves (Whitehead, 1961; Axford, 1963; Chimonas and Axford, 1968). Additional studies by Fujitaka and Tohmatsu (1973), Wilkinson et al. (1992), and Szuszczewicz et al. (1995), based on ionosonde data, established the importance of the tidal wave (TW) influence on Es. The Es dynamics control by TWs was investigated also by Haldoupis et al. (2006), who proposed a new methodology named height-time-intensity (HTI), which has been recently used also by Pignalberi et al. (2014) and Oikonomou et al. (2014).

More recently, it has been recognized also the importance of planetary waves (PWs), that set up a horizontal wind-shear mechanism causing a plasma accumulation in areas of positive vorticity, as formulated by Shalimov et al. (1999) and Shalimov and Haldoupis (2002), and then verified by Haldoupis and Pancheva (2002) and Pancheva et al. (2003). These kind of waves are global oscillations of neutral atmosphere at periods of about 2, 5, 10 and 16 days, also called Rossby normal modes (Holton, 1975; Forbes, 1995). They are mainly of tropospheric origin and can penetrate directly to height slightly above 100 km as it was theoretically proposed by Charney and Drazin (1961), and Dickinson (1968), and experimentally verified by Pancheva and Mukhtarov (2000).

Haldoupis et al. (2004) found an amplitude modulation, with periods of days, of the diurnal periodicity characterizing the Es critical frequency of the ordinary mode of propagation (*fo*Es) time series, and they associated this phenomenon to a nonlinear interaction between TWs and PWs concurrently present at low altitudes. Similar results were also found by Sauli and Bourdillon (2008) and Pignalberi et al. (2015). This nonlinear wave interaction was formulated by Teitelbaum and Vial (1991) and verified in neutral atmospheric winds studies (Beard et al., 1999; Pancheva et al., 2000; Pancheva, 2000; Pancheva and Mukhtarov, 2000).

This paper is based on *fo*Es measurements recorded at the ionospheric station of Rome (41.8°N, 12.5°E), Italy, over the years from 1976 to 2009, a period of time including the solar cycles 21, 22, and 23.

This work shows and discusses the fact that the amplitude modulation characterizing the *fo*Es diurnal periodicity is greater for high solar activity than for low solar activity. Section 2 describes how the data analysis has been carried out and illustrates the corresponding results. The discussion of the results and the conclusions are the subject of Section 3.

2. Data analysis and results

The data set considered in this study is constituted by hourly values of *fo*Es recorded at the ionospheric station of Rome (Italy, 41.8°N, 12.5°E) from 1976 to 2009, a period of time including three solar cycles, with 4 minima and 3 maxima of solar activity. The whole data set was validated according to the URSI (International Union of Radio Science) standard (Piggott and Rawer, 1972). Data were downloaded from the electronic Space Weather upper atmosphere (eSWua) database (http://www.eswua.ingv.it/) (Romano et al., 2008). As indicator of the solar activity the index $F_{10.7}$ is considered, and Table 1 shows the maximum and minimum values of $F_{10.7}$ of the solar cycles involved in our analysis.

It must be underlined that during the analyzed period there was no change of ionosonde from the classical one to the DPS4 digisonde (Bibl and Reinisch 1978), which could have led to a significant decrease of *fo*Es average values (Lastovicka et al., 2012). The *fo*Es values were all validated from traces recorded by classical ionosondes, which cannot tag the different polarization characterizing the two different modes of propagation of the electromagnetic wave. A VOS-1 chirp ionosonde produced by the Barry Research Corporation, Palo Alto, CA, USA (Barry Research Corporation, 1975) sounded from January 1976 to November 2004, and then it was replaced by an AIS-INGV ionosonde (Zuccheretti et al., 2003). This means that the *fo*Es validated time series considered in this study represent a reliable and homogeneous data set.

Specifically, *fo*Es hourly values between the 4 June at 00:00 UT and the 28 August at 07:00 UT, were considered for each year, both because it is known that Es layer is most pronounced in summertime (e.g. Haldoupis et al., 2007; Pietrella and Bianchi, 2009; Pignalberi et al., 2014), and also because in this way the available values for each year are 2048, a multiple of 2, which is a constraint of the wavelet transform algorithm used in our study, to avoid *edge problems* and *cut problems*. Another constraint of the wavelet transform algorithm is the completeness of the time series; this is why the *fo*Es data gaps, caused by the absence of the layer, were filled with the corresponding monthly mean values. However, for each of the considered years, for the period June-August, the cases of ionograms not showing the presence of an Es layer are few; with regard to this issue, the reader can refer to the eSWua database and view (after registering) the *fo*Es daily plots of June, July, and August, of the "Rome Validated Data" section, for all the years from 1976 to 2009. Table 2 shows the occurrence percentage of the various types of Es traces, *f*(lat), *l*(ow), *c*(usp) and *h*(igh), recorded between the 4 June at 00:00 UT and the 28 August at 07:00 UT, for the whole data set from 1976 to 2009.

The Continuous Wavelet Transform (CWT) technique was employed to obtain a temporal characterization of the periodicities imprinted in *fo*Es, and it was applied for some years of low and high solar activity to explore a possible dependence on solar cycle variability. The corresponding wavelet spectrograms of Fig. 1 show that, for all the considered years, *fo*Es is characterized both by a diurnal periodicity and by a semidiurnal periodicity, with the former which is by far better-defined than the latter; moreover, the diurnal periodicity appears more intense for years of high solar activity (see the years 1981, 1989, 1990, and 2000) than for years of low solar activity (see the years 1987, 1996, and 2009). Fig. 1 shows also the appearance of periodicities that correspond more or less to the normal Rossby modes of planetary waves. Specifically, the spectrograms show: significant periodicities between 5 and 10 days for the low solar activity years 1976, 1986, 1987, 1996, and for the high solar activity years 1981, 1989, 2000; significant periodicities between 10 and 16 days for the low solar activity years 1976, 1986, 1997, and for the high solar activity years 1981, 2000; significant periodicities greater than 16 days for the low solar activity years 1996, 1997, and for the high solar activity years 1981, 1986, 1989, 1990, 2000, 2001. Overall, Fig. 1 shows that PW periodicity amplitudes are more intense for high solar activity than for low solar activity (with regard to this, one can compare for instance the periodicities between 5 and 10 days of the years 1981 and 2000 with the corresponding ones of the years 1976 and 1996, especially from day 155 to about day 200). Figure 1 shows also that the diurnal periodicity is amplitude modulated, with a period of several days, and an interesting feature pointed out by Fig. 1 is that this amplitude modulation is greater for high solar activity (see the years 1989, 1990, and 2000) than for low solar activity (see the years 1987, 1996, 2009).

To deeper investigate how the *fo*Es is affected by tidal and planetary periodicities, amplitude spectra of the *fo*Es time series of each considered year, for periodicities between 2 and 36 h, and for periodicities between 1.5 and 20 days, were respectively computed through a Fast Fourier Transform (FFT) spectral analysis and a Windowed Fourier Transform (WFT) spectral analysis. The different choice of spectral analysis is because the two wave phenomena have different characteristics. It is known in fact that tidal waves influence continuously Es layers with diurnal and semidiurnal periodicities (Haldoupis et al., 2004, 2006) and then can be considered as a stationary phenomenon; on the contrary, planetary waves influence Es layers only for a definite time (typically of a few weeks) with periods similar to those of the normal Rossby modes, and then they can be considered as transient phenomena. Figures 2, 3, and 4 show the results of the aforementioned analyses for the years 1996, 2000, and 2009, respectively. These figures show that the *fo*Es time series presents a pronounced diurnal variability, with the corresponding 72 h running mean (the red tick line in Figs. 2a, 3a, and 4a) which is amplitude modulated with periods from a few to several days; moreover, as expected, the FFT amplitude spectra (Figs. 2b, 3b, and 4b) are dominated by two narrow spectral peaks at 12 and 24 h that greatly exceed the 95% level of confidence independently of the solar activity. The WFT amplitude spectra of Figs. 2c, 3c, and 4c, show instead that PW periodicities embedded in the *fo*Es time series depend on the solar activity; in fact, by comparing the 1996 and 2000 WFT spectra, one sees that the peak amplitudes are greater in 2000, which is a year of high solar activity, but most of all the WFT spectrum of 2009 (a year of prolonged low solar activity) shows no peak exceeding the 95% level of confidence. The same feature is also perceivable by looking at the 72 h running means of Figs. 2a, 3a, and 4a that present and amplitude modulation which is high in 2000 (high solar activity), lower in 1996 (low solar activity), and almost absent in 2009 (prolonged low solar activity).

3. Discussion and conclusions

The CWT spectrograms of Fig. 1 show that, for all the considered years, the *fo*Es characteristic presents a well-defined diurnal periodicity. This is quite expected, since the Es layer is characterized by a daily cycle, due to the photoionization process caused by the Sun radiation, for which the daytime layer is usually stronger than the nighttime one. However, the *fo*Es diurnal periodicity visible both in Fig. 1, and also in the FFT spectra of Figs. 2b, 3b, and 4b, is also due to the influence that tidal waves have on the vertical wind-shear mechanism, on which the Es formation is based (Lindzen and Chapman, 1969; Fujitaka and Tohmatsu, 1973; Wilkinson et al., 1992; Mathews et al., 1993; Forbes, 1995; Szuszczewicz et al., 1995; Haldoupis, 2011, 2012; Pignalberi et al., 2014). Hence, actually, the clear 24 h periodicity characterizing the *fo*Es time series is due to a mixing of two causes: the photoionization process triggered by the Sun which causes the Es daily cycle, and the effect that tidal waves have on the Es layer, through the wind-shear mechanism.

At the same time, Fig. 1 shows also the appearance of periodicities that correspond more or less to the normal Rossby modes of planetary waves. Figure 1 shows that PW periodicity amplitudes are more intense for high solar activity than for low solar activity; for instance, if we compare the periodicities between 5 and 10 days of the years 1981 and 2000 (years of high solar activity) with the corresponding ones of the years 1976 and 1996 (years of low solar activity), we can see that the corresponding intensities are higher for high solar activity than for low solar activity, especially from day 155 to about day 200. This feature is strengthened by the WFT spectral plots of Figs. 2c, 3c, and 4c, calculated on the *fo*Es time series of years 1996, 2000, and 2009, showing that the higher the solar activity the higher the PW peak amplitudes; concerning this, the most striking feature highlighted by the WFT plots is the absence of peaks exceeding the 95% level of confidence in 2009, a year of prolonged low solar activity.

With regard to Fig. 2 it is worth noting that the corresponding results are very similar to those shown in the Fig. 1 of Haldoupis et al. (2004), although the analyses are based on data recorded at different ionospheric stations. In particular, Haldoupis et al. (2004) showed that, besides the dominant and known 24 h and 12 h tidal periodicities, there is also a weaker terdiurnal (8-hour) oscillation embedded in the *fo*Es time series, and they interpreted the amplitude modulation suffered by these three periodicities in terms of the nonlinear interaction between tidal waves and planetary waves. Also the FFT spectrum of Fig. 2b, alike the one shown in the Fig. 1 of Haldoupis et al. (2004), shows a terdiurnal oscillation which is above the 95% level of confidence, confirming that also this periodicity can affect the Es dynamics. The present work is however focused on the 24 h periodicity, the 12 h and the 8 h periodicities are out of the scope of the analysis here described.

The amplitude modulation suffered by the diurnal periodicity, with periods of several days, and experimentally pointed out both by Haldoupis et al. (2004) and by Pignalberi et al. (2015), is significantly highlighted in Fig. 1, as well as in Figs. 2a, 3a, and 4a. According to the theory of Teitelbaum and Vial (1991), this amplitude modulation is caused by a nonlinear interaction between tidal and planetary waves. As demonstrated by Teitelbaum and Vial (1991), besides modulating the signal amplitude, the nonlinear interaction mechanism gives also rise to secondary waves, causing in the spectrum the appearance of sidebands around the TW periodicity, for frequencies equal to the sum and difference of the primary wave interacting frequencies. In order to look for these secondary peaks, according to Pignalberi et al. (2015), FFT spectra were calculated on *fo*Es time series associated to the diurnal periodicity, that were extracted and filtered from the corresponding spectrograms shown in Fig 1, according to the following two steps: (a) the wavelet coefficients with periods from 20 to 28 h were selected; (b) the inverse wavelet transform was applied to these coefficients in order to extract the signal related to the diurnal periodicity. Figure 5 shows the FFT amplitude spectrum, for periods ranging from 16 to 32 h, of the *fo*Es diurnal time series extracted and filtered from the spectrogram of 2000 of Fig.1, according to the aforementioned two steps. This figure points out that additionally to the primary peak due to the diurnal TW, there are secondary peaks exceeding the 95% level of confidence, the most important of which have been highlighted with arrows of different colors: the green ones at about 23 and 25.2 h are consistent with a nonlinear interaction between the diurnal TW and a PW with a period of about 18 days; the red ones at about 21.9 and 27 h are consistent with a nonlinear interaction between the diurnal TW and a PW with a period of about 9-10 days; the blue ones at about 19.4 and 31.6 h are consistent with a nonlinear interaction between the diurnal TW and a PW with a period of about 4-5 days. Figure 6, which is the same as Fig. 5 but for 2009, shows that there are no secondary coupled peaks exceeding the 95% level of confidence. Hence, Figs. 5 and 6 point out two important points: 1) the amplitude modulation visible in Fig. 1, 2a, 3a, and in the first part of the Fig. 4a, is certainly caused by a nonlinear interaction between tidal waves and planetary waves; 2) the nonlinear interaction between tidal waves and planetary is strongly dependent on the solar activity.

The fact that the amplitude characterizing the modulation of the diurnal periodicity is greater for high solar activity than for low solar activity is clearly visible also in Fig. 1, where for instance the years 1989, 1990, and 2000 (years of high solar activity), show an amplitude modulation which is greater than that characterizing the years 1987, 1996, and 2009 (years of low solar activity).

This feature could be finally explained with a positive correlation between the PW activity and the solar cycle variability, as described by Jacobi (1998), and as it is also evident by looking at

Figs. 2c, 3c, and 4c which clearly show as the energy associated to the planetary waves is more important during periods of high solar activity than for low solar activity.

Ultimately, this work shows beyond any doubt that the Es layer, in terms of the corresponding amplitude modulation caused by a TW-PW nonlinear interaction, depends on solar activity.

References

Axford, W. I., 1963. The formation and vertical movement of dense ionized layers in the ionosphere due to neutral wind shears, J. Geophys. Res., 68 (3), 769-779.

Barry Research Corporation, 1975. VOS-1A User Manual, Palo Alto, California, USA.

Beard, A. G., Mitchell, N., Williams, P. J. S. Kunitake, M., 1999. Nonlinear interactions between tides and planetary waves resulting in periodic tidal variability, J. Atmos. Sol. Terr. Phys., 61, 363-376.

Bibl, K., Reinisch, B.W, 1978. The universal digital ionosonde, Radio Sci., 13, 519–530, doi: 10.1029/RS013i003p00519.

Charney, J. G., Drazin, P. G., 1961. Propagation of planetary-scale disturbances from the lower into the upper atmosphere, J. Geophys. Res., 66 (1), 83-109.

Chimonas, G., Axford, W. I., 1968. Vertical movement of temperate-zone sporadic E layers, J. Geophys. Res., 73 (1) , 111-117.

Dickinson, R. E., 1968. On the exact and approximate linear theory of vertically propagating planetary Rossby waves forced at a spherical lower boundary, Monthly Weather Review, 96 (7), 405-415.

Forbes, J. M., 1995. Tidal and planetary waves, in: The upper Mesosphere and lower Thermosphere, a review of experiment and theory, edited by: Johnson R.M., and Killen T.L., 67-87, Geophysical Monograph 87, American Geophysical Union.

Fujitaka, K., Tohmatsu, T., 1973. A tidal theory of the ionospheric intermediate layer, J. Atmos. Terr. Phys., 35, 425-438.

Haldoupis, C., Pancheva, D., 2002. Planetary waves and midlatitude sporadic E layers: strong experimental evidence for a close relationship, J. Geophys. Res., 107 (A6), http://dx.doi.org/10.1029/2001JA000212, SIA 3-1-SIA 3-6.

Haldoupis, C., Pancheva, D., Singer, W., Meek, C., Mac-Dougall, J., 2007. An explanation for the seasonal dependence of midlatitude sporadic E layers, J. Geophys. Res., 112, A06315, doi:10.1029/2007JA012322.

Haldoupis, C., Pancheva, D., Mitchell, N. J., 2004. A study of tidal and planetary wave periodicities present in midlatitude sporadic E layers, J. Geophys. Res., 109, A02302, doi:10.1029/2003JA010253.

Haldoupis, C., Meek, C., Christakis, N., Pancheva, D., Bourdillon, A., 2006. Ionogram height-time intensity observations of descending E layers at mid-latitude, J. Atmos. Sol.-Terr. Phys., 68, 539-557, doi:10.1016/j.jastp.2005.03.020.

Haldoupis, C., 2011. A tutorial review on Sporadic E layers, in the book: Aeronomy of the Earth's Atmosphere–Ionosphere, chapter 29, 381-394, IAGA Book Series Volume 2, Springer.

Haldoupis, C., 2012. Midlatitude Sporadic E layers. A typical paradigm of atmosphere-ionosphere coupling, Space Sci. Rev., 168, 441-461, http://dx.doi.org/10.107/s 11214-011-9786-8.

Holton, J. R., 1975. The dynamic meteorology of the stratosphere and mesosphere, in: Meteorological Monographs, 15, American Meteorological Society, Boston, 218 pp..

Jacobi, C., 1998. On the solar cycle dependence of winds and planetary waves as seen from mid-latitude D1 LF mesopause region wind measurements, Ann. Geophysicae, 16, 1534 -1543.

Lastovicka, J., Boska, J., Buresova, D., Kouba, D., 2012. High historical values of foEs – reality or artefact?, J. Atmos. Sol. Terr. Phys., 74, 51–54.

Lindzen, R. S., Chapman, S., 1969. Atmospheric Tides, Space Sci. Rev., 10, 3–188.

Mathews, J. D., Morton, Y. T., Zhou, Q., 1993. Observations of ion layer motions during the AIDA campaign, J. Atmos. Terr. Phys., 55, 447–457.

Mathews, J. D., 1998. Sporadic E: current views and recent progress, J. Atmos. Sol.-Terr. Phys., 60 (4), 413-435.

Oikonomou, C., Haralambous, H., Haldoupis, C., Meek, C., 2014. Sporadic E tidal variabilities and characteristics observed with the Cyprus Digisonde, J. Atmos. Sol. Terr. Phys., 119, 173-183, doi:10.1016/j.jastp.2014.07.014.

Pancheva, D., 2000. Evidence for nonlinear coupling of planetary waves and tides in the lower thermosphere over Bulgaria, J. Atmos. Sol. Terr. Phys., 62, 115-132.

Pancheva, D., Mukhtarov, P., Mitchell, N. J., Beard, A. G., Muller, H. G., 2000. A comparative study of winds and tidal variability in the mesosphere/lower-thermosphere region over Bulgaria and the UK, Ann. Geophys., 18, 1304-1315.

Pancheva, D., Mukhtarov, P., 2000. Wavelet analysis on transient behavior of tidal amplitude fluctuations observed by meteor radar in the lower thermosphere above Bulgaria, Ann. Geophys., 18, 316-331.

Pancheva, D., Mitchell, N., Middleton, H., Muller, H., 2003. Variability of the semidiurnal tide due to fluctuations in solar activity and total ozone, J. Atmos. Solar. Terr. Phys., 65, 1-19.

Piggott, W.R., Rawer, K., 1972. URSI handbook of ionogram interpretation and reduction, US Department of Commerce, National Oceanic and Atmospheric Administration, Environmental Data Service, Asheville, NC, 326, Report UAG 23.

Pignalberi, A., Pezzopane, M., Zuccheretti, E., 2014. Sporadic E layer at mid-latitudes: average properties and influence of atmospheric tides, Ann. Geophys., 32, 1427-1440, www.ann-geophys.net/32/1427/2014/.

Pignalberi, A., Pezzopane, M., Zuccheretti, E., 2015. A spectral study of the mid-latitude sporadic E layer characteristic oscillations comparable to those of the tidal and the planetary waves, J. Atmos. Sol. Terr. Phys., 122, 34-44, http://dx.doi.org/10.1016/j.jastp.2014.10.017.

Pietrella, M., Bianchi, C., 2009. Occurrence of sporadic-E layer over the ionospheric station of Rome: analysis of data for thirty-two years, Adv. Space Res., 44,72-81. http://dx.doi.org/10.1016/j.asr.2009.03.006.

Romano, V., Pau, S., Pezzopane, M., Zuccheretti, E., Zolesi, B., De Franceschi, G., Locatelli, S., 2008. The electronic Space Weather upper atmosphere (eSWua) project at INGV:

Advancements and state of the art. Ann. Geophys. 26, 345-351, doi:10.5194/angeo-26-345-2008.

Sauli, P., Bourdillon, A., 2008. Height and critical frequency variations of the sporadic-E layer at midlatitudes. J. Atmos. Sol.–Terr. Phys. 70, 1904–1910. http: //dx.doi.org/10.1016/j.jastp.2008.03.016.

Shalimov, S., Haldoupis, C., Voiculescu, M., Schlegel, K., 1999. Midlatitude E region plasma accumulation driven by planetary wave horizontal wind shears, J. Geophys. Res., 104 (A12), 207-213.

Shalimov, S., Haldoupis, C., 2002. A model of mid-latitude E region plasma convergence inside a planetary wave cyclonic vortex, Ann. Geophys., 20, 1193-1201.

Szuszczewicz, E. P., Roble, R. G., Wilkinson, P. J., Hanbaba, R., 1995. Coupling mechanisms in the lower ionospheric - thermospheric system and manifestations in the formation and dynamics of intermediate descending layers, J. Atmos. Terr. Phys., 57, 1483-1496.

Teitelbaum, H., Vial, F., 1991. On tidal variability induced by nonlinear interaction with planetary waves, J. Geophys. Res., 96, 14169-14178.

Whitehead, J. D., 1961. The formation of the sporadic-E layer in the temperate zones, J. Atmos. Terr. Phys., 20, 49-58.

Whitehead, J.D., 1989 Recent work on mid-latitude and equatorial sporadic-E, J. Atmos. Terr. Phys., 51 (5), 401-424.

Wilkinson, P. J., Szuszczewicz, E. P., Roble, R. G., 1992. Measurements and modelling of intermediate, descending, and sporadic layers in the lower ionosphere: results and implications for global-scale ionospheric- thermospheric studies, Geophys. Res. Lett., 19 (2), 95-98.

Zuccheretti, E., Tutone, G., Sciacca, U., Bianchi, C., Arokiasamy, B. J., 2003. The new AIS-INGV digital ionosonde, Ann. Geophys. Italy, 46, 647–659.

Table 1. Months of lowest and highest solar activity for solar cycles 21, 22, 23, and 24 with the corresponding value of the solar index $F_{10.7}$.

Solar Cycle	Lowest Solar Activity	Highest Solar Activity
21	Jun 1976 ($F_{10.7}$ = 72.7)	Dec 1979 ($F_{10.7}$ = 207.5)
22	Sep 1986 ($F_{10.7}$ = 72.8)	Jul 1989 ($F_{10.7}$ = 201.4)
23	May 1996 ($F_{10.7}$ = 69.6)	Apr 2000 ($F_{10.7}$ = 164.7)
24	Dec 2008 ($F_{10.7}$ = 64.9)	

Table 2. The occurrence percentage of the various types (f, l, c and h) of Es recorded between the 4 June at 00:00 UT and the 28 August at 07:00 UT, for the whole data set from 1976 to 2009.

Total Ionograms	Ionograms with Es	Es type "*c*"	Es type "*h*"	Es type "*l*"	Es type "*f*"
65003	57123	25131 (~44%)	1368 (~3%)	7736 (~13%)	22888 (~40%)

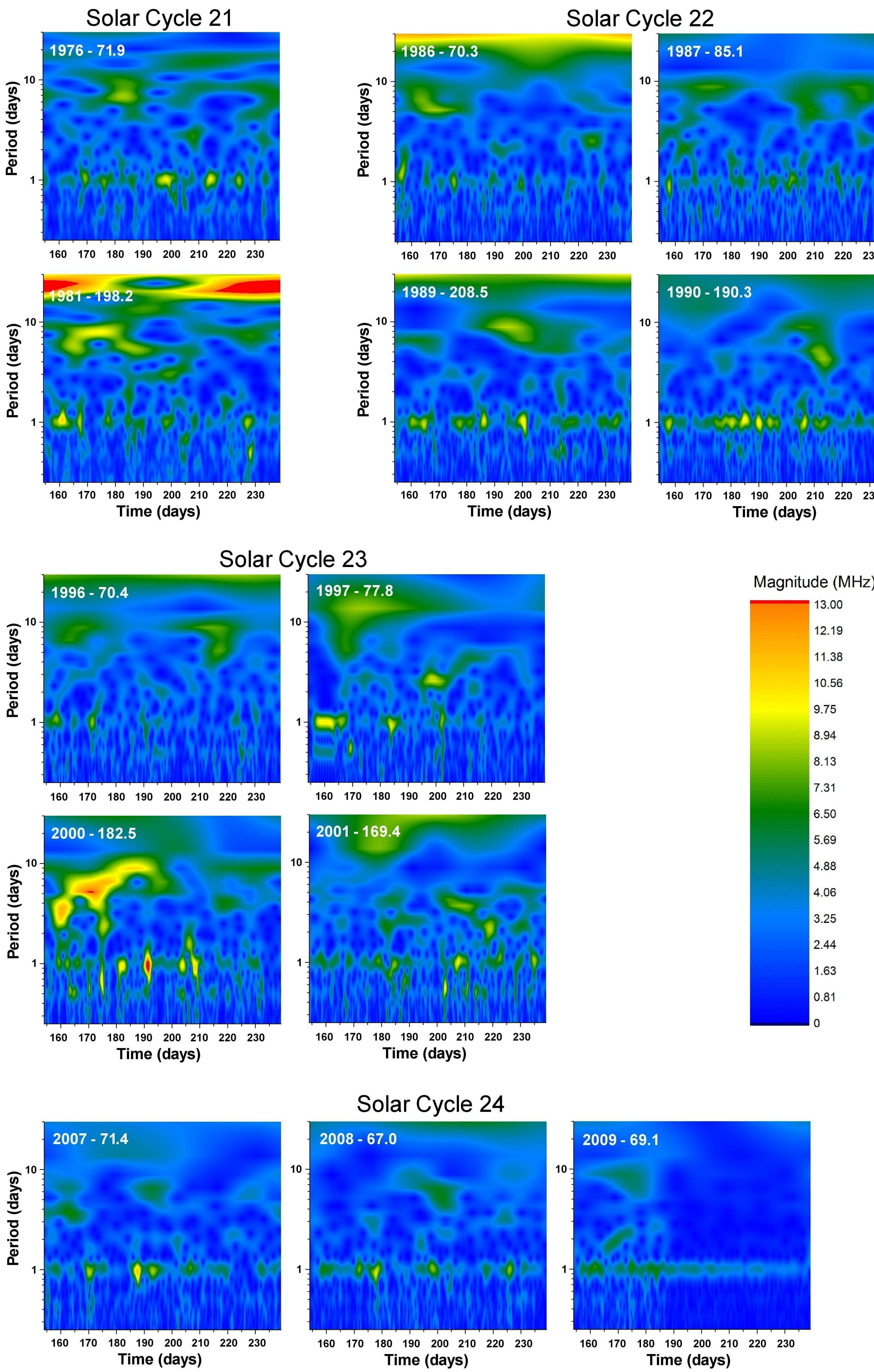
Solar Cycle 21
1976 - 71.9
1981 - 198.2
Solar Cycle 22
1986 - 70.3
1987 - 85.1
1989 - 208.5
1990 - 190.3
Solar Cycle 23
1996 - 70.4
1997 - 77.8
2000 - 182.5
2001 - 169.4
Solar Cycle 24
2007 - 71.4
2008 - 67.0
2009 - 69.1
Period (days)
Time (days)
1
10
160 170 180 190 200 210 220 230
Magnitude (MHz)
13.00
12.19
11.38
10.56
9.75
8.94
8.13
7.31
6.50
5.69
4.88
4.06
3.25
2.44
1.63
0.81
0

Figure 1. CWT spectrograms, grouped by solar cycle, of the *fo*Es hourly values recorded between the day 155 at 00:00 UT and the day 240 at 07:00 UT for some years of low solar activity (1976, 1986, 1987, 1996, 1997, 2007, 2008, and 2009) and high solar activity (1981, 1989, 1990, 2000, and 2001), for periods ranging from a few hours to 30 days. In the upper left corner of each spectrogram, the corresponding year and yearly mean value of $F_{10.7}$ are typed. Horizontal dashed white lines highlight the tidal periodicities at 12 and 24 h. Horizontal dashed black lines highlight planetary periodicities at 2, 5, 10, and 16 days.

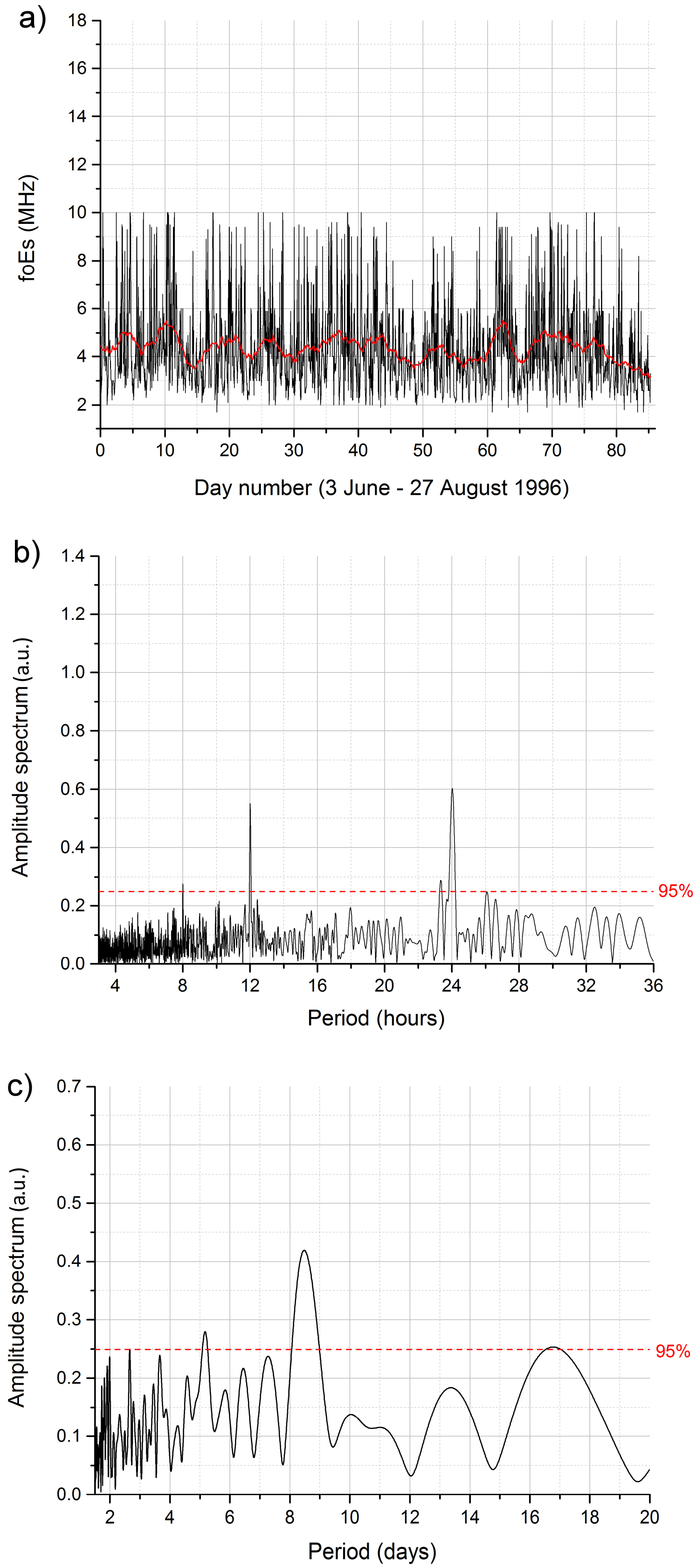
a)
foEs (MHz)
Day number (3 June - 27 August 1996)
b)
Amplitude spectrum (a.u.)
95%
Period (hours)
c)
Amplitude spectrum (a.u.)
95%
Period (days)

Figure 2. (a) *fo*Es hourly values recorded at Rome from 4 June 1996 at 00:00 UT to 28 August 1996 at 07:00 UT (the tick red line represents the 72 h running mean). (b) FFT amplitude spectrum of the *fo*Es time series shown in (a) for periods ranging between 3 and 36 h. (c) WFT amplitude spectrum of the *fo*Es time series shown in (a) for periods ranging between 1.5 and 20 days. The horizontal dashed lines in (b) and (c) indicate the corresponding 95% level of confidence.

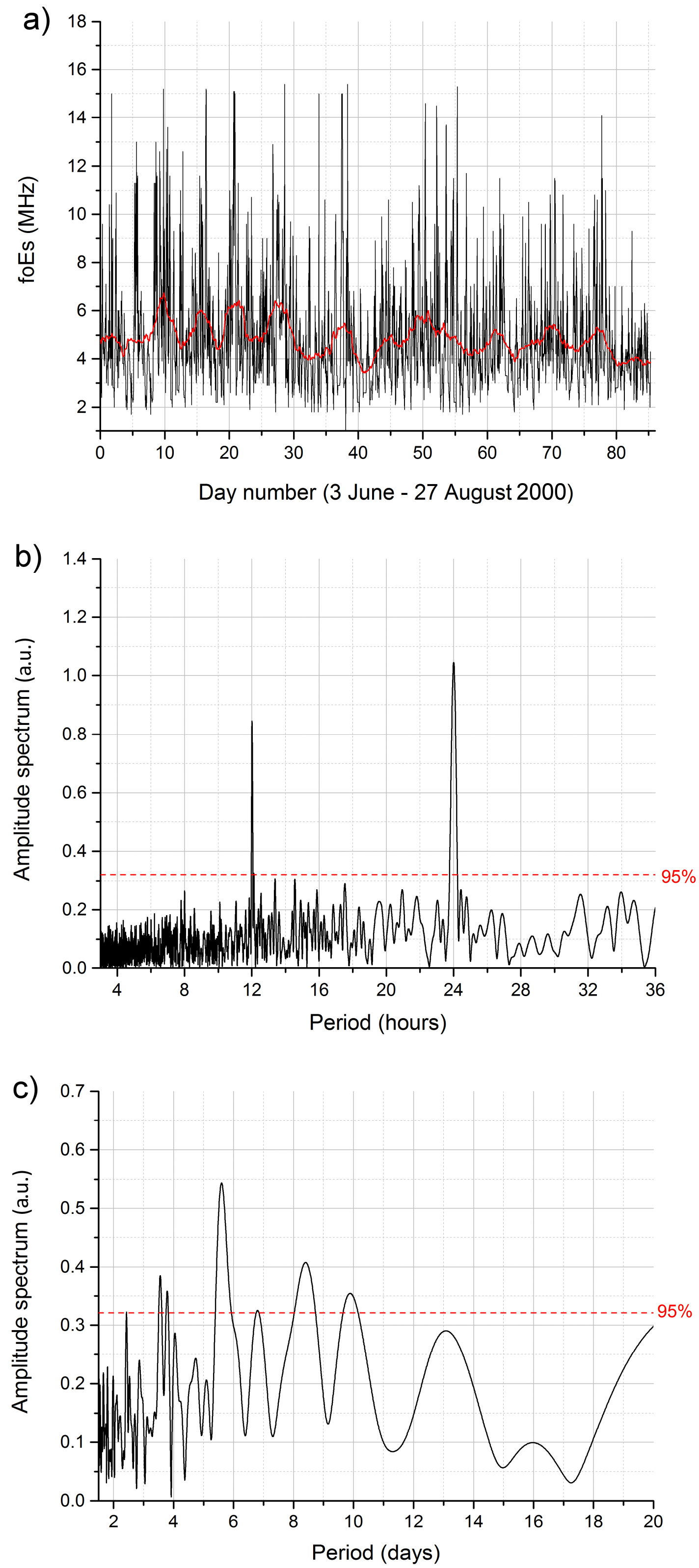

Figure 3. Same as Fig. 2 but for the year 2000.

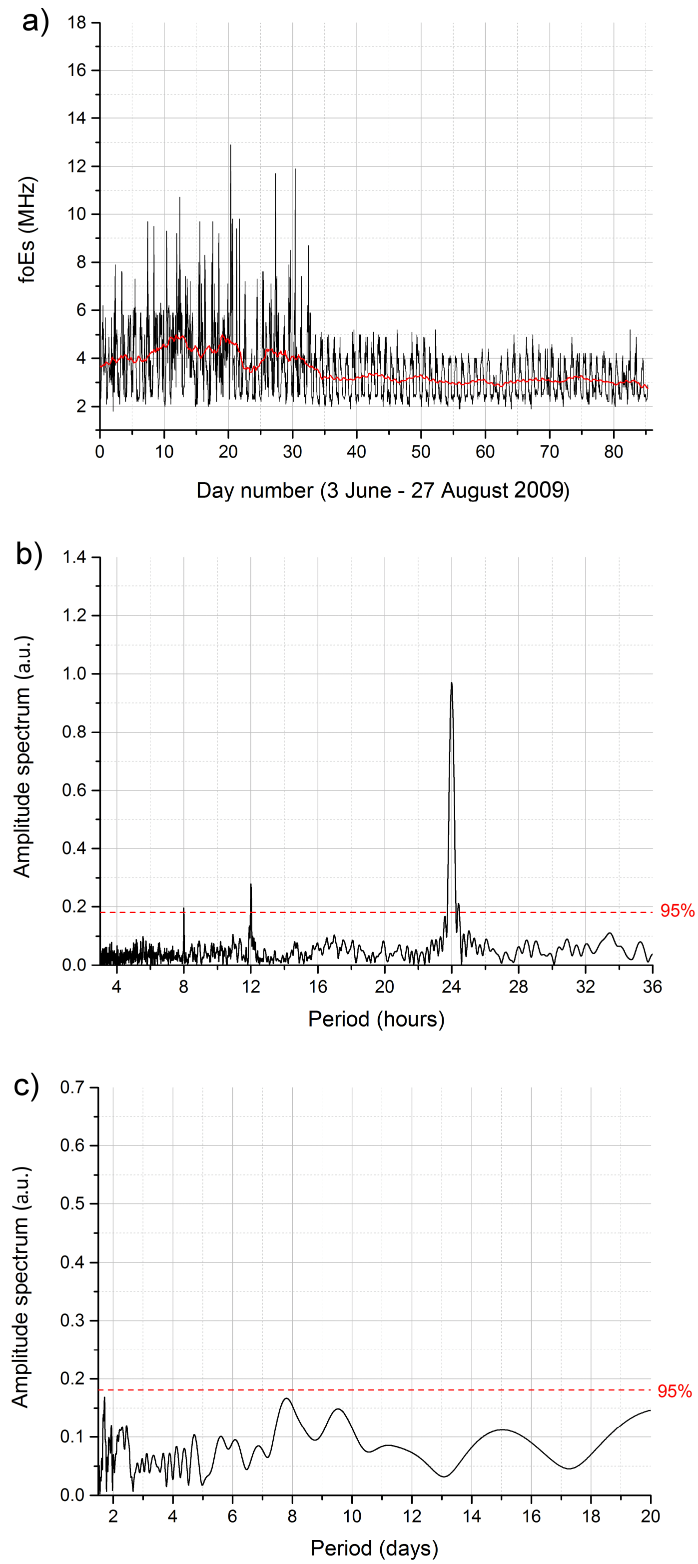

Figure 4. Same as Fig. 2 but for the year 2009.

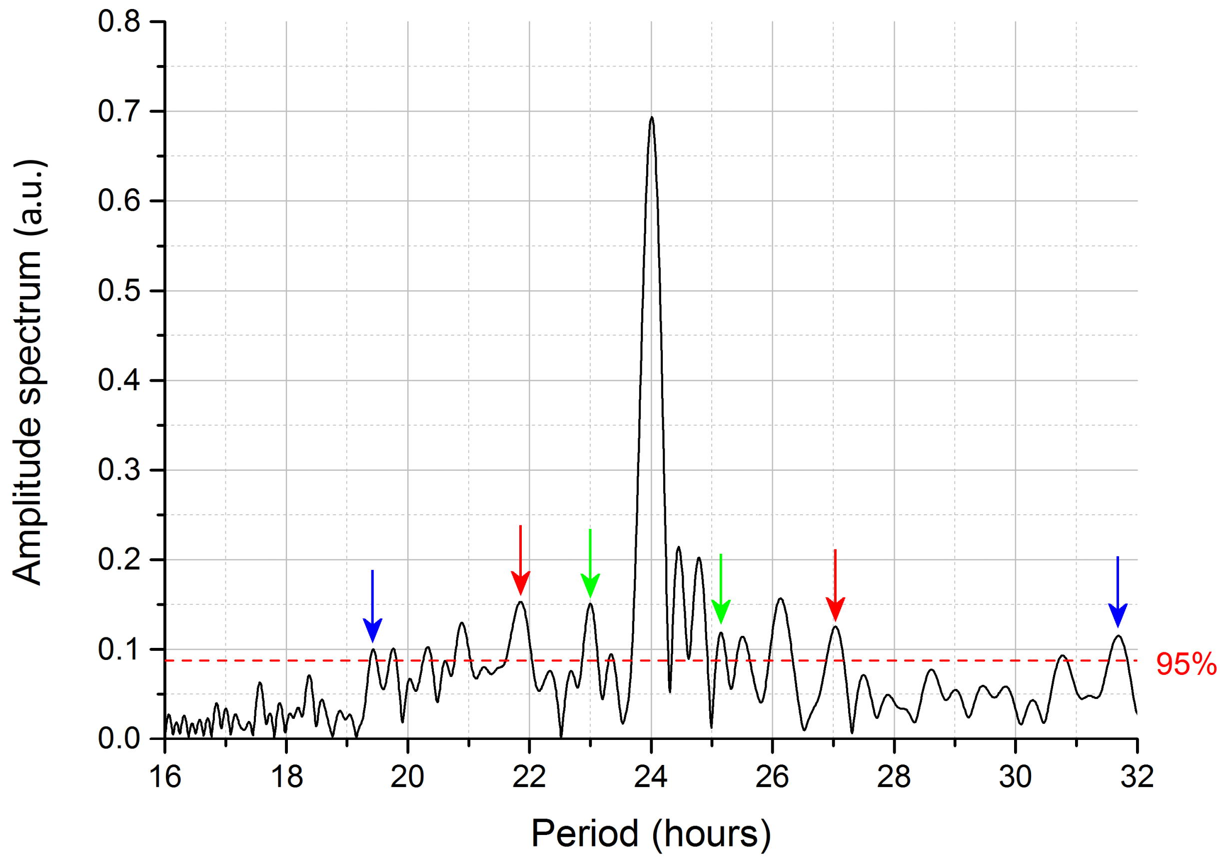

Figure 5. FFT amplitude spectrum, for periods ranging from 16 to 32 h, calculated on the *fo*Es time series associated to the diurnal periodicity, that was extracted and filtered from the corresponding spectrograms of year 2000 of Fig. 1, according to the method described in Pignalberi et al. (2015).

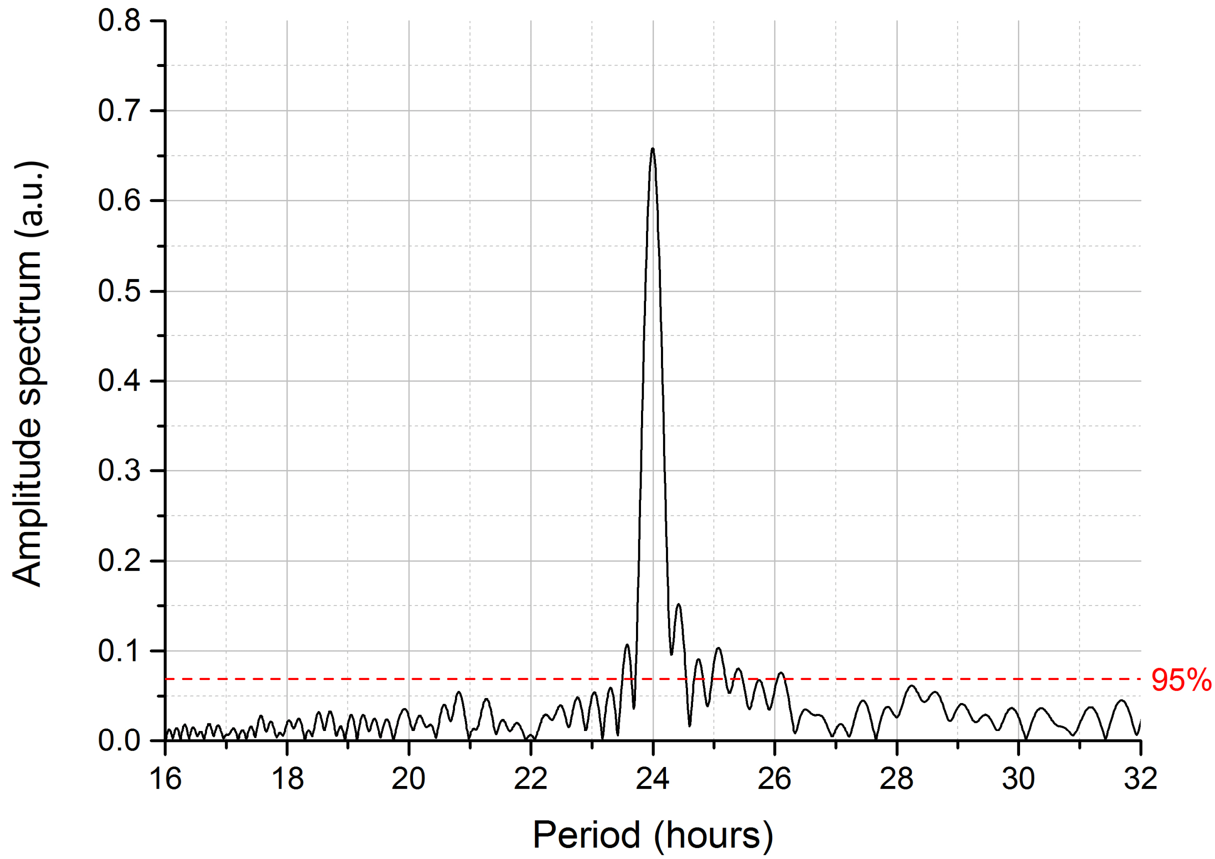

Figura 6. Same as Fig. 5 but for the year 2009.